



Article

Degradation Characteristics of Carbon Tetrachloride by Granular Sponge Zero Valent Iron

Xueqiang Zhu ^{1,*}, Yuncong Li ², Baoping Han ³, Qiyan Feng ¹ and Lai Zhou ¹

¹ School of Environmental Science and Spatial Informatics, China University of Mining and Technology, Xuzhou 221116, China; fqycumt@126.com (Q.F.); zhoulai99@cumt.edu.cn (L.Z.)

² Department of Soil and Water Sciences, Tropical Research and Education Center, University of Florida, Homestead, FL 33031, USA; yunli@ufl.edu

³ School of Geography & Geomatics and Urban-Rural Planning, Jiangsu Normal University, Xuzhou 221116, China; bphan@cumt.edu.cn

* Correspondence: zhuxq0615@163.com; Tel.: +86-138-1329-0158

Abstract: Granular sponge zero valent iron (ZVI) was employed to degrade carbon tetrachloride (CCl₄). The effects of acidic washing, initial solution pH, and ZVI dosage on CCl₄ degradation were investigated. Results showed that CCl₄ was effectively removed by ZVI and approximately 75% of CCl₄ was transformed into chloroform through hydrogenolysis. The rate of chloroform transformation was slower compared to that of CCl₄, resulting in chloroform accumulation. CCl₄ degradation was a pseudo first-order process. The observed pseudo first-order reaction rate constant (k_{obs}) for CCl₄ and chloroform were 0.1139 and 0.0109 h⁻¹, respectively, with a ZVI dosage of 20 g/L and an initial CCl₄ concentration of 20 mg/L. Surface acidic washing had a negligible effect on CCl₄ degradation with ZVI. The k_{obs} for CCl₄ degradation increased linearly with increasing ZVI dosage and the optimal dosage of ZVI was 20 g/L based on the surface area-normalized rate constants. The negative relationship between k_{obs} and the solution pH indicated that the degradation of CCl₄ by ZVI performed better under weakly acidic conditions.

Keywords: granular sponge iron; carbon tetrachloride; reductive dechlorination; chloroform



Citation: Zhu, X.; Li, Y.; Han, B.; Feng, Q.; Zhou, L. Degradation Characteristics of Carbon Tetrachloride by Granular Sponge Zero Valent Iron. *Int. J. Environ. Res. Public Health* **2021**, *18*, 12578. <https://doi.org/10.3390/ijerph182312578>

Academic Editor: Paul B. Tchounwou

Received: 3 November 2021

Accepted: 27 November 2021

Published: 29 November 2021

Publisher's Note: MDPI stays neutral with regard to jurisdictional claims in published maps and institutional affiliations.



Copyright: © 2021 by the authors. Licensee MDPI, Basel, Switzerland. This article is an open access article distributed under the terms and conditions of the Creative Commons Attribution (CC BY) license (<https://creativecommons.org/licenses/by/4.0/>).

1. Introduction

Carbon tetrachloride (CCl₄) has been used for a variety of purposes, including as a dry-cleaning solvent, metal degreaser, pesticide, refrigerant, fire extinguisher, flame retardant, and intermediate for industrial products [1]. Massive use, improper disposal and emission of CCl₄ have caused severe soil and groundwater pollution [2,3]. CCl₄ is the most common soil-groundwater contaminant [4], which poses a serious threat to ecological and human health and is found in at least 430 of the 1662 NPL sites [5]. In the 200 West Area of the U.S. Department of Energy Hanford Site, as much as 580 m³ CCl₄ may have been released into groundwater [6]. CCl₄ is a potential human carcinogen and has been identified as a priority pollutant by the Ministry of Environmental Protection of China, U.S. Environment Protection Agency and the European Commission [7]. The presence of CCl₄ in groundwater is a major concern due to its toxicity, environmental persistence and widespread presence [8]. Therefore, remediation of CCl₄-contaminated groundwater is of great significance.

Zero valent iron (ZVI) is an excellent electron donor capable of reductive transformation of contaminants with E_h^0 greater than -0.44 V ($Fe^0 \rightarrow Fe^{2+} + 2e^-$, $E^0 = -0.44$ V) [9]. ZVI has been widely applied to remediation of sites contaminated by chlorinated hydrocarbons, heavy metals, nitrate and polycyclic aromatic hydrocarbons [10]. Compared to microscale iron particles, nano zero valent iron (nZVI) has a higher reactivity towards a variety of contaminants. The increase in the reactivity of nZVI particles mainly results from the increased reactive surface areas [11]. However, the reactivity of ZVI highly depends on the

amount of reactive surface area since the degradation of contaminants by ZVI is a surface area reaction; the specific surface area normalized reaction rate constants for chlorinated hydrocarbons degradation with microscale zero-valent iron (mZVI) particles are in the same order of magnitude as obtained with nZVI particles, while mZVI corrosion rate is much slower [12]. In addition, mZVIs removed chlorinated aliphatic hydrocarbons more effectively than nZVIs when the ZVI material was used singly for field applications according to 112 field case studies provided in the literatures [13]. Recently, less expensive mZVI particles have been developed as a substitute for nZVIs to effectively degrade chlorinated hydrocarbons because of the high cost of nZVI and shortened lifetime due to high surface reactivity and fast corrosion rate with water [13–15]. The objective of this work was to evaluate the effectiveness of the highly porous sponge ZVI micro-particles in reducing CCl_4 under laboratory conditions. The impacts of various parameters, including acid washing, ZVI dosage, and initial solution pH on CCl_4 reduction were evaluated. Changes in concentrations of CCl_4 and the intermediate products were monitored to identify the reaction mechanism.

2. Materials and Methods

2.1. Experiment Procedure

Irregular-shaped sponge iron particles used in this work were purchased from Tianjin Zhongcheng Iron Powder Factory (Tianjin, China). The material had a mean grain size less than $150\ \mu\text{m}$ and a specific surface area of $0.078\ \text{m}^2/\text{g}$ [16]. The composition of the ZVI including Fe (96.52%), O (2.4%), Si (0.5%), Mn (0.29%), Ca (0.13%), Cr (0.048%), Mg (0.043%), P (0.038%), and S (0.031%) was analyzed using S8-TIGER X-ray Fluorescence (Bruker Corporation, Germany). The sponge iron particles (0.5 kg) were washed with 1.5 L of 0.1 mol/L H_2SO_4 in a 2 L beaker by mixing and stirring at 300 r/min for 0.5 h, and then rinsed with 1.5 L of ultrapure water for 0.5 h for five times. CCl_4 was analytical reagent grade and purchased from the Sinopharm Chemical Reagent Company (Shanghai, China).

Batch experiments of CCl_4 degradation by ZVI were conducted on a rotary shaker of $200 (\pm 5)\ \text{r/min}$ at $25 (\pm 0.2)\ ^\circ\text{C}$. Acid-washed and non-acid-washed ZVIs (2 g) were placed in 100 mL serum vials with 100 mL deionized water, and 100 μL of $2 \times 10^4\ \text{mg/L}$ CCl_4 was added to form the test solution with the initial CCl_4 concentration of 20 mg/L. The $2 \times 10^4\ \text{mg/L}$ CCl_4 solution was prepared by dissolving 12.5 μL CCl_4 in 1 mL methanol and diluting to 10 mL with deionized water. Samples were taken at reaction times of 1, 4, 8, 16, 24, 48, 72 and 96 h for the analysis of CCl_4 and its degradation products concentrations.

2.2. Analysis and Data Processing

The mass concentrations of CCl_4 , CHCl_3 , and CH_2Cl_2 were analyzed using an Agilent 6890N Gas Chromatograph (Agilent Technologies Inc., Santa Clara, CA, USA) equipped with a micro-cell electron capture detector and a G1888 Headspace Sampler and a 30 m long HP-5 capillary column. The temperature conditions were: oven temperature of $30\ ^\circ\text{C}$, injection port temperature of $150\ ^\circ\text{C}$, detector temperature of $250\ ^\circ\text{C}$. Separation was conducted with a temperature program: initial oven temperature $30\ ^\circ\text{C}$ hold for 1 min, then ramped at $1\ ^\circ\text{C}/\text{min}$ to $80\ ^\circ\text{C}$ and hold for 1 min. Ultrapure nitrogen was used as a carrier gas for the GC with a flow rate of 2 mL/min (split ratio 10:1).

The surface morphology of ZVI was analyzed by a Quanta 250 environmental scanning electron microscope (FEI, Hillsboro, OR, USA) equipped with a QUANTAX 400-10 electric refrigeration spectrometer (Bruker, Germany).

The kinetics of the reductive dechlorination of CCl_4 by ZVI can be described by a pseudo first-order reaction kinetic model [17].

$$\frac{dC_{CT}}{dt} = -k_{obs}C_{CT} \quad (1)$$

where C_{CT} is the concentration of CCl_4 at a certain time and k_{obs} is the observed pseudo first-order reaction rate constant.

Studies showed that the reductive dechlorination rate constant is usually insensitive to changes in the initial concentrations of chlorinated hydrocarbons (e.g., trichloroethene concentrations of 1.21–61 mg/L) [18]. Therefore, the pseudo first-order reaction kinetic model is applicable to the reductive dechlorination of chlorinated hydrocarbons with concentrations within a typical concentration range.

The reductive dechlorination of CCl_4 by ZVI is a surface reaction, and the dechlorination rate of CCl_4 depends on the effective surface area of ZVI. Therefore, the reductive dechlorination kinetics of CCl_4 can also be expressed by the surface-area-normalized rate constant [19].

$$\frac{dC_{CT}}{dt} = -k_{SA}a_s\rho_m C_{CT} = -k_{SA}\rho_a C_{CT} \quad (2)$$

where k_{SA} is the surface-area-normalized rate constant ($\text{L}/(\text{h}\cdot\text{m}^2)$), a_s is the specific surface area (m^2/g) of ZVI, ρ_m is the mass concentration of ZVI (g/L), and ρ_a is the surface area concentration of ZVI (m^2/L). The k_{SA} , calculated using the equation $k_{SA} = k_{obs}/\rho_a$, is independent of ZVI, the mass, specific surface area, and volume of the reaction solution. Due to its small range of variation, k_{SA} is more suitable for the characterization of ZVI reactivity and the comparison of reactivity between different materials, compared with k_{obs} . Equation (2) shows that the pseudo first-order reaction rate constant increases with the specific surface area of the material, which also means that the performance of the material can be improved by reducing the size of the material at the limited reaction range. However, as fine particulate materials typically possess low permeability, a balance has to be struck between reactivity and permeability in filed applications.

3. Results and Discussion

3.1. Effect of Acid-Washing Pretreatment on CCl_4 Removal

Theoretically, oxides can be removed from the surface of ZVI particles through acid-washing, which increases the surface area of ZVI particles and facilitates the reductive dechlorination of chlorinated hydrocarbons by ZVI particles [20]. However, experimental studies show that pretreated ZVI is less effective in Cr(VI) removal as compared to untreated ZVI. This may be due to the fact that acid-washing leads to more severe mineral precipitation on the ZVI surface, thereby reducing the reactivity and long-term effectiveness of ZVI [21]. In our experiment, the reductive dechlorination of CCl_4 by acid-washed and non-acid-washed ZVI was compared (Figure 1). Results showed that the relative concentration of CCl_4 in the blank control group was 93.7% after 48 h and 90.1% after 72 h. The small reduction may be caused by volatilization. In addition, ZVI has low adsorption capacity and selectivity for targeted contaminants, especially for organic contaminants [22]. Xin et al. found that the amount of TCE removed by adsorption of XG-mZVI (the specific surface area is $0.136 \pm 0.024 \text{ m}^2/\text{g}$) was 1.80–2.08 μg and the amount of TCE removed by chemical reduction was 94.55–127.50 μg after 480 h reaction under different conditions [23]. The adsorption capacity of ZVI increases with the decrease in the particle size and the specific surface area of mZVI used in our study was only $0.078 \text{ m}^2/\text{g}$. Therefore, it is believed that the adsorption of CCl_4 on mZVI in our study can be ignored. In subsequent experiments, the loss of CCl_4 caused by volatilization and adsorption on ZVI particles was ignored. The efficiency of CCl_4 degradation by acid-washed ZVI was similar to that of non-acid-washed ZVI, with the respective rates of CCl_4 removal being 87.4% and 82.7% after 16 h, and 96.6% and 95.9% after 24 h. These results indicated that acid-washing pretreatment did not significantly change the reductive dechlorination capability of ZVI on CCl_4 , and the respective observed pseudo first-order reaction rate constants under experimental conditions were 0.1167 h^{-1} and 0.1139 h^{-1} .

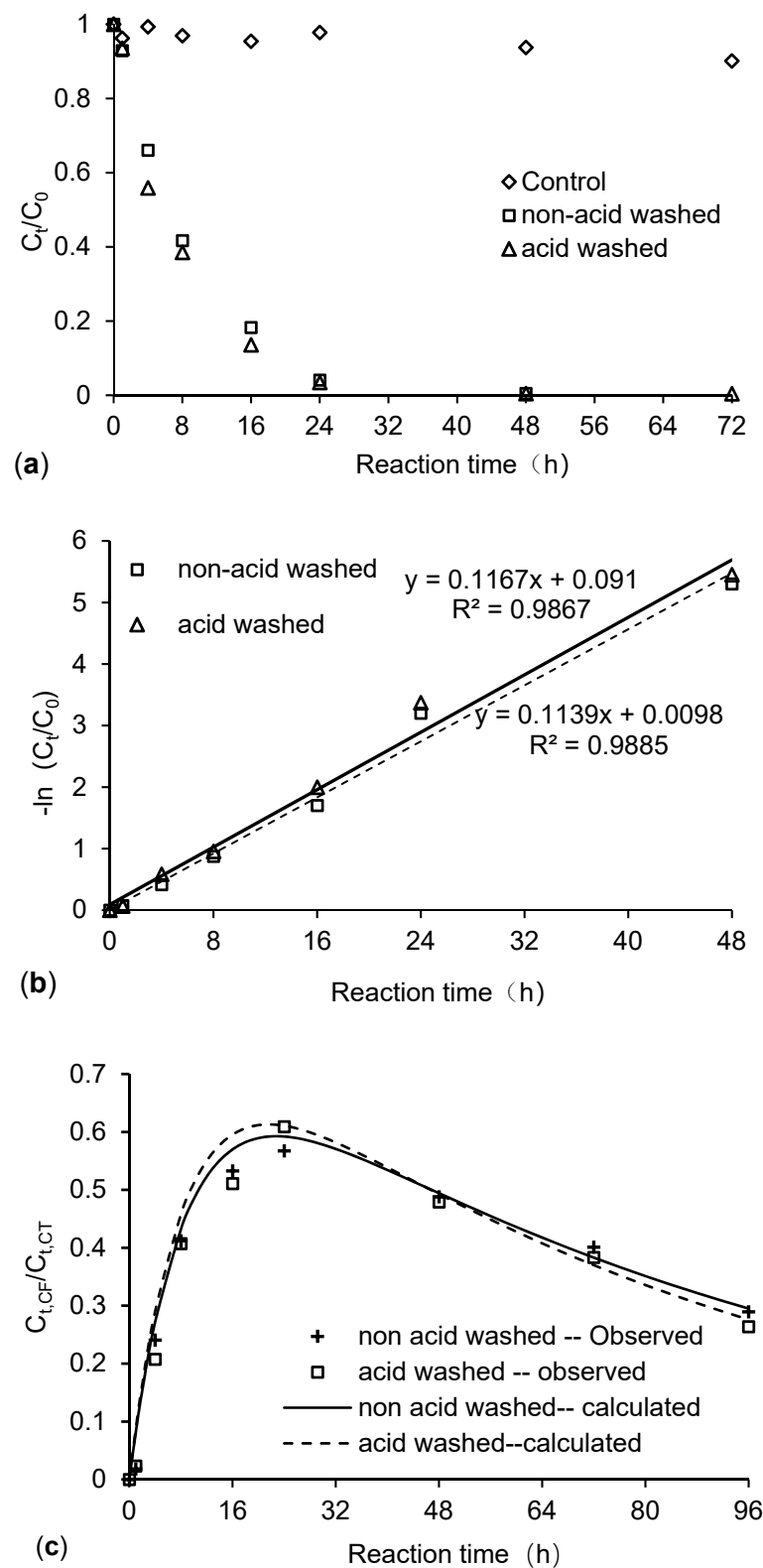


Figure 1. CCl_4 degradation by acid-washed and non-acid washed ZVIs under the conditions of ZVI dosage of 20 g/L, initial CCl_4 concentration of 20 mg/L, initial solution pH of 7 and stirring rate of 200 r/min. (a) Changes in CCl_4 concentration with time, (b) degradation kinetics of CCl_4 . (c) Changes in concentration of chloroform with time. C_0 was the initial CCl_4 concentration, C_t was the CCl_4 concentration at time t, and $C_{t,CF}$ was the $CHCl_3$ concentration at time t.

The purpose of acid-washing was to remove the oxidation film on the ZVI particle surface. As shown in Figure 2, SEM results indicated that non-acid-washed ZVI particles had rough surfaces with a large number of pores, while acid-washed ZVI particles had smoother surfaces. The ZVI surface structure did not change significantly after acid-washing, and the EDS results indicated the absence of O (or the O content was below the detection limit) for both acid-washed and non-acid-washed ZVI. Therefore, it can be deduced that ZVI particles had a lower oxide coverage before and after acid-washing, which indicated that acid-washing pretreatment had no significant effect on the efficiency and rate of the reductive dechlorination of CCl₄. Hence, in subsequent experiments, ZVI was unwashed.

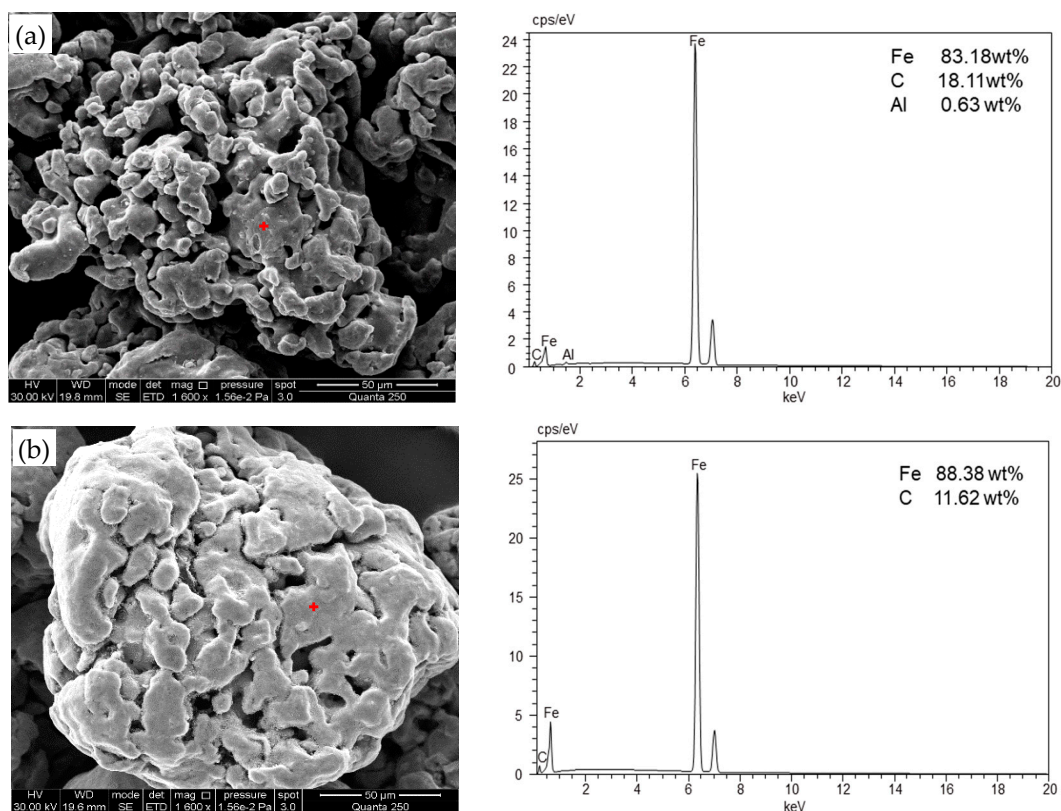


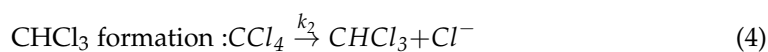
Figure 2. SEM images of ZVI: (a) acid-washed ZVI, (b) non-acid washed ZVI.

During the degradation of CCl₄, only chloroform (CHCl₃, CF) was detected, while dichloromethane was not detected. As shown in Figure 1, the CHCl₃ concentration increased gradually as CCl₄ concentration decreased, with peak concentration occurring 24 h after the start of the reaction. When the degradation of CCl₄ was complete, the CHCl₃ concentration began to decrease.

3.2. Reaction Kinetics of Reductive Degradation of CCl₄ by ZVI

Figure 3 displays that CCl₄ degradation can be represented by a consecutive first-order reaction process. The concentrations of CCl₄ and CHCl₃ at any time can be expressed using Equations (3)–(7) [24,25].

$$\text{CCl}_4 \text{ degradation : } [\text{CCl}_4]_t = [\text{CCl}_4]_0 e^{-k_1 t} \tag{3}$$



$$[\text{CHCl}_3]_t = \alpha [\text{CCl}_4]_0 (1 - e^{-k_1 t}); \alpha = \frac{k_2}{k_1} \tag{5}$$

$$\text{CHCl}_3 \text{ degradation} : \frac{d[\text{CHCl}_3]_t}{dt} = \alpha k_1 [\text{CCl}_4]_0 - k_3 [\text{CHCl}_3]_t \tag{6}$$

$$\text{CHCl}_3 \text{ concentration} : [\text{CHCl}_3]_t = \frac{k_2 [\text{CCl}_4]_0}{k_3 - k_1} (e^{-k_1 t} - e^{-k_3 t}) \tag{7}$$

where $[\text{CCl}_4]_t$ and $[\text{CHCl}_3]_t$ are the concentrations of CCl_4 and CHCl_3 at time t ; $[\text{CCl}_4]_0$ is the initial concentration of CCl_4 ; k_1 is the overall pseudo first-order reaction constant for CCl_4 ; k_2 is the formation constant for CHCl_3 ; k_3 is the transformation constant for CHCl_3 ; and α is the fraction of CCl_4 transformed to CHCl_3 .

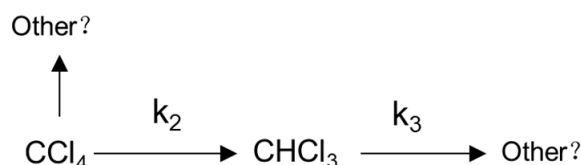


Figure 3. Reductive degradation mechanism of CCl_4 .

Table 1 and Figure 2 show the fitting results of the observed pseudo first-order reaction of CCl_4 and CHCl_3 degradation by ZVI. It was obvious that the CHCl_3 removal capacity in the ZVI- H_2O system was significantly lower than the CCl_4 removal capacity. The redox potential of $\text{CHCl}_3/\text{CCl}_4$ ($E^0 = 0.673 \text{ V}$) is higher compared to the $\text{CH}_2\text{Cl}_2/\text{CHCl}_3$ ($E^0 = 0.560 \text{ V}$) [26], which indicates that highly chlorinated aliphatic hydrocarbons are more easily reduced than species with a lower number of chlorine atoms [27]. Thus, the lower chlorinated hydrocarbons such as CHCl_3 may accumulate in CCl_4 plumes. The observed reaction rate constant for CHCl_3 was approximately 10% as compared to CCl_4 , meaning that CHCl_3 existed in the ZVI system for longer.

Table 1. The apparent reaction rate constants for CCl_4 and chloroform degradation by acid and non-acid washed ZVI.

Reaction Medium	k_1 (h^{-1})	k_2 (h^{-1})	k_3 (h^{-1})	α
Acid washed ZVI	0.1167	0.0931	0.0122	0.7980
Non-acid washed ZVI	0.1139	0.0865	0.0109	0.7569

The ratio of CCl_4 transformed to CHCl_3 was less than 1.00 (0.7980 and 0.7569, respectively), indicating the presence of other competing reactions during the reductive dechlorination of CCl_4 , such as reductive hydrolysis that generates dichlorocarbene or chloroform free radicals. This is a characteristic of the CCl_4 reductive dechlorination reaction [28].

3.3. Effect of ZVI Dosage on Reductive Dechlorination of CCl_4

Figure 4 shows that CCl_4 removal efficiency increases with the increase of ZVI dosage. After 16 h, the CCl_4 removal rate in the system with a ZVI dosage of 5 g/L was only 42.2%, while the removal rate was 95.4% when the ZVI dosage was 40 g/L. After 48 h, CCl_4 removal rates with ZVI dosages ranging from 5–40 g/L were 79.6%, 98.7%, 99.5%, 99.5%, and 99.5%, respectively, indicating that CCl_4 could be completely removed when the initial concentration of ZVI exceeded 10 g/L. The reductive dechlorination of CCl_4 by ZVI is a surface-mediated reaction; therefore, the dechlorination rate of CCl_4 strongly depends on the effective surface areas. The number of effective active reaction sites in the ZVI- H_2O system changes with ZVI dosage. A higher dosage of ZVI can provide more available reactive sites for CCl_4 dechlorination and subsequently enhance the degradation of CCl_4 [29].

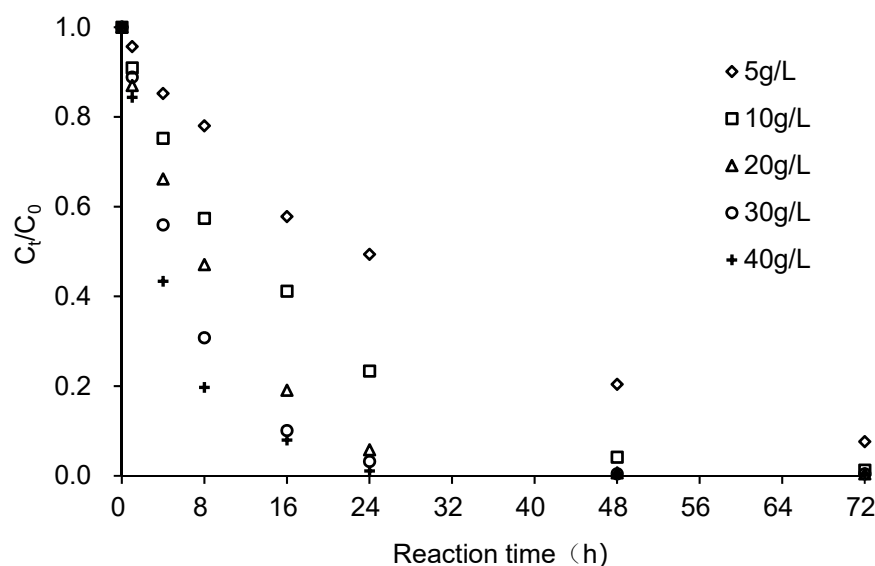


Figure 4. Effect of ZVI dosage on the degradation of CCl₄. Reaction conditions were: ZVI dosage of 5, 10, 20, 30, and 40 g/L, CCl₄ initial concentration of 20 mg/L, initial solution pH of 7 and stirring rate of 200 r/min. C₀ was the initial CCl₄ concentration and C_t was the CCl₄ concentration at time t.

Figure 5 demonstrates the reaction kinetics of the reductive dechlorination of CCl₄ at different ZVI dosages (the relevant parameters are not listed). When the ZVI dosages were 5, 10, 20, 30, and 40 g/L, the observed pseudo first-order reaction rate constants (k_{obs}) of CCl₄ degradation were 0.0325, 0.0649, 0.1058, 0.1437, and 0.1788 h⁻¹, respectively. Results indicate that k_{obs} increased linearly with ZVI dosage, with the trend line fitted to Equation (8).

$$k_{obs} = 0.0041ZVI_{dosage} + 0.0194, R^2 = 0.9914 \tag{8}$$

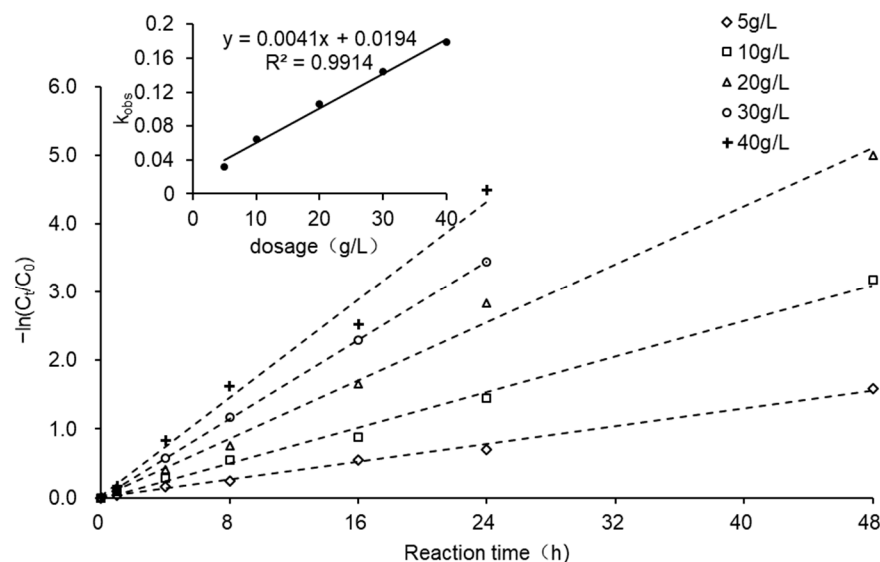


Figure 5. Reaction kinetics for CCl₄ reductive dechlorination by ZVI with different dosages.

The specific surface area of ZVI was 0.078 m²/g. The k_{SA} values for ZVI dosages of 5, 10, 20, 30, and 40 g/L, obtained by converting k_{obs} into the surface-area-normalized reaction rate, were 0.0833, 0.0832, 0.0678, 0.0614, and 0.0573 L/(h \times m²), respectively. Contrasting with k_{obs} , k_{SA} decreased as the dosage increased, suggesting that sufficient active reaction sites were provided by the system when the dosage was over 20 g/L. Therefore, a ZVI dosage of 20 g/L was used in the subsequent experiments.

Figure 6 reveals that the relative concentration of CHCl_3 increases initially and then subsequently decreases; the peak time occurred earlier as the ZVI dosage increases. When ZVI dosages were 30 and 40 g/L, peak CHCl_3 concentrations occurred at 16 h. Conversely, when the ZVI dosage was 10 g/L, the peak CHCl_3 concentration occurred at 48 h and when ZVI was 5 g/L, the peak CHCl_3 concentration occurred after 72 h. However, experimental results also showed that the peak concentration of CHCl_3 did not change significantly with changes in ZVI dosage with the range of 0.592–0.637. The ratio of CCl_4 transformed to CHCl_3 varied within the range of 0.729–0.763 under different ZVI dosages, indicating that a varied dosage only changed the CCl_4 degradation rate, while the degradation pathway of CCl_4 by ZVI was not altered.

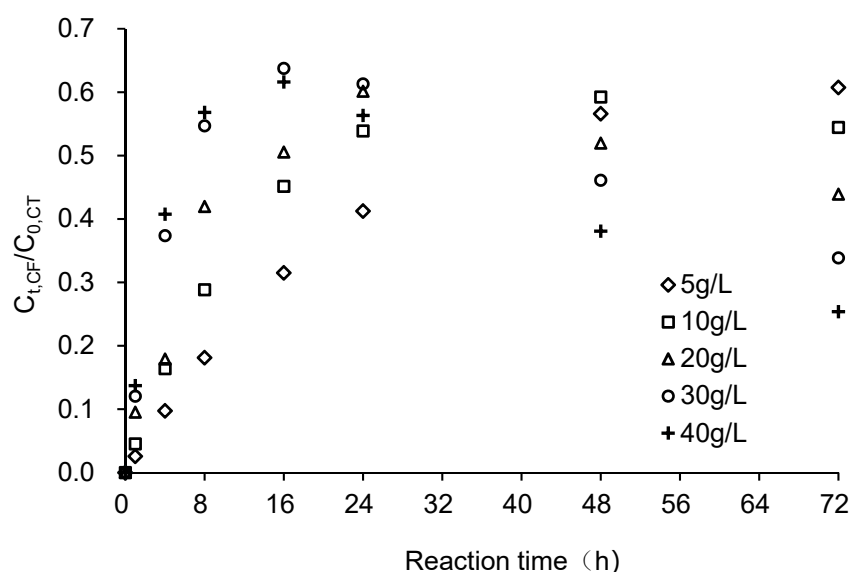


Figure 6. Changes in CF concentration at different dosages of ZVI. $C_{0,CT}$ was the initial CCl_4 concentration and $C_{t,CF}$ was the CHCl_3 concentration at time t .

3.4. Effect of Initial Solution pH on Reductive Dechlorination of CCl_4

The pH of the reaction solution can promote corrosion or passivation of ZVI, and the redox half-reaction of chlorinated hydrocarbons ($\text{RCl} + 2e^- + \text{H}^+ \rightarrow \text{RH} + \text{Cl}^-$, $E^0 = 0.5\text{--}1.5$ V when $\text{pH} = 7$) indicates that H^+ is directly involved in the reductive dechlorination of chlorinated hydrocarbons. Therefore, pH is an important factor influencing the reductive dechlorination of CCl_4 by ZVI. As described in Figure 7, pH had a considerable influence on CCl_4 removal. After 8 h, CCl_4 removal rates at pH values of 5, 6, 7, and 8 were 72.1%, 69.6%, 59.7%, and 50.0%, respectively, and after 48 h CCl_4 removal rates exceeded 99.0% in all cases. Jiao et al. showed that the lower pH accelerated the dechlorination reaction of CCl_4 with ZVI [30]. Shih et al. reported that decreasing pH from 9.3 to 3.2 resulted in an increase in pseudo first-order reaction constants of hexachlorobenzene by nZVI from 0.052 h^{-1} to 0.12 h^{-1} [31]. Figure 8 shows the pseudo first-order reaction kinetics of CCl_4 degradation at different pH values. It was apparent that the degradation of CCl_4 by ZVI at different pH values corresponded to pseudo first-order reaction kinetics. The k_{obs} decreased with increasing pH, with the trend line fitted to Equation (9).

$$k_{obs} = -0.0239 \text{ pH} + 0.2837, R^2 = 0.9684 \quad (9)$$

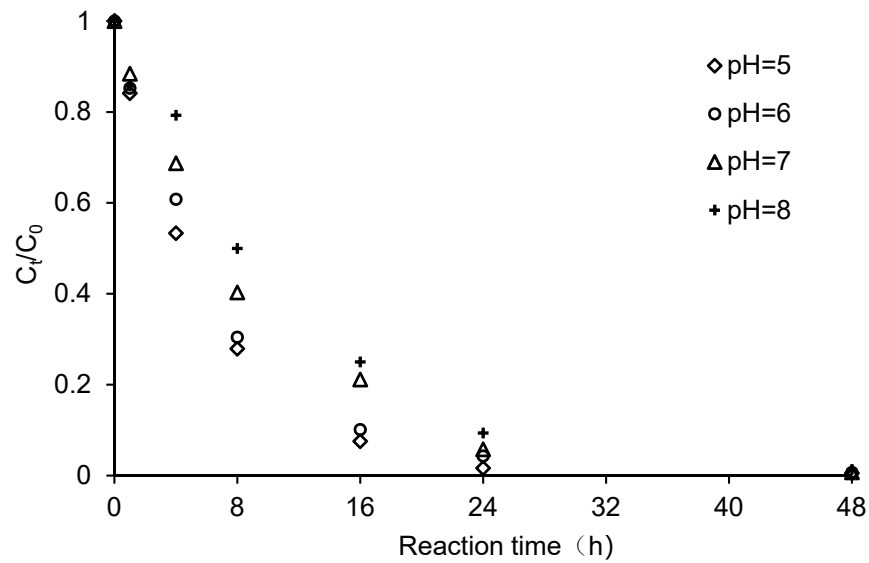


Figure 7. Effect of pH on CCl₄ degradation by ZVI. Reaction conditions were: Initial solution pH of 5, 6, 7 and 8, ZVI dosage of 20 g/L, CCl₄ initial concentration of 20 mg/L, stirring rate of 200 r/min. C₀ was the initial CCl₄ concentration and C_t was the CCl₄ concentration at time t.

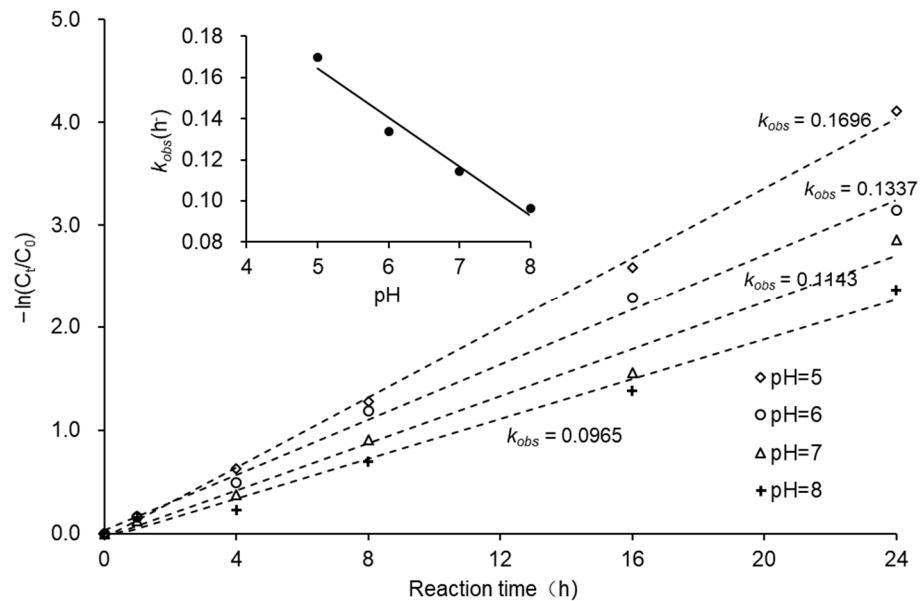
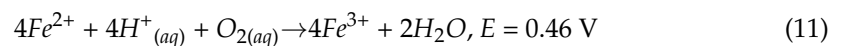
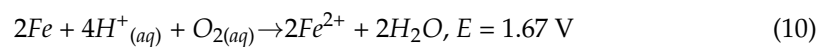


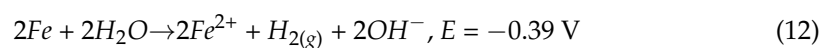
Figure 8. Reaction kinetics for CCl₄ degradation at different initial solution pH.

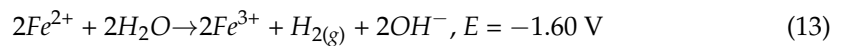
The influence of initial pH on the reductive dechlorination of CCl₄ can be attributed to the participation of H⁺ during the reaction. Moreover, lower solution pH is linked to accelerated ZVI corrosion [32] and prevention of the formation of passivation layer on ZVI surface [33]. The electrochemical corrosion process of ZVI in the solution can be expressed as follows [34]:

Under acidic conditions:



Under neutral and alkaline conditions:





Therefore, under weakly acidic conditions, sufficient H^+ could be provided by the system for ZVI corrosion, leading to the steady generation of H_2 for CCl_4 degradation [35]. Under low pH conditions, ferrous hydroxide and other passivation films were also prevented from accumulating on ZVI surfaces, thereby creating more active reaction sites [36]. Moreover, low pH also promoted Fe^{2+} release and adsorption on the ZVI surfaces. The Fe^{2+} adsorbed on the mineral surfaces promoted the transfer of electrons from ZVI to CCl_4 , which in turn promoted the reductive dechlorination of CCl_4 [37]. Under alkaline conditions, a series of complex iron hydroxide ions (such as $[\text{Fe}(\text{OH})]^+$, $[\text{Fe}(\text{OH})_3]^-$, and $[\text{Fe}(\text{OH})_4]^{2-}$) may have been formed on the ZVI surfaces, thereby inhibiting the reductive dechlorination reaction.

3.5. Significance of the Experimental Results on Permeable Reactive Barrier Design

One of the key factors considered in permeable reactive barrier (PRB) design is the residence time required for contaminants to reach the target concentrations, which generally determine the thickness of the PRB. Because contaminant degradation occurs within the PRB, in addition to considering the concentration of the target contaminants, it is also necessary to consider the degradation pathways of the contaminants and their intermediate products when determining the appropriate residence time. The required thickness of the PRB can be estimated by Equations (14) and (15) using the reaction rate constants of contaminant degradation, groundwater flow rates of the contaminated site, and the control concentrations of the target contaminants [38].

$$b = v \times t_{ref} \times SF \quad (14)$$

$$t_{res} = \frac{-\ln \frac{C_t}{C_0}}{k_{obs}} \quad (15)$$

where b is the PRB thickness, v is the flow rate of groundwater in the reaction medium, t_{res} is the residence time of the contaminant, SF is the safety factor, C_0 is the initial contaminant concentration, C_t is the target contaminant concentration downstream of the PRB, and k_{obs} is the reaction rate constant of contaminant degradation.

Supposing that the initial concentrations of CCl_4 and CHCl_3 in the groundwater in a specific contaminated site were $1000.0 \mu\text{g/L}$ and $0.0 \mu\text{g/L}$, respectively, the values for the transformation parameters of CCl_4 and CHCl_3 in the ZVI- H_2O system could be obtained from the results in Table 1. Using Equations (3)–(7), the concentration of CCl_4 and CHCl_3 for different residence times are described in Figure 9. After 27 h, CCl_4 concentration decreased from $1000.0 \mu\text{g/L}$ to $57.0 \mu\text{g/L}$, while CHCl_3 concentration increased from $0.0 \mu\text{g/L}$ to $460.5 \mu\text{g/L}$ before decreasing gradually. According to China's Standards for Drinking Water Quality (GB5749-2006), the maximum allowable concentrations of CCl_4 and CHCl_3 are $2.0 \mu\text{g/L}$ and $60.0 \mu\text{g/L}$, respectively. In order to achieve the control targets, if CCl_4 was considered on its own, the minimum residence time of contaminants in the PRB would be 59 h, and the concentrations of CCl_4 and CHCl_3 would be $1.9 \mu\text{g/L}$ and $377.2 \mu\text{g/L}$, respectively. If CCl_4 and CHCl_3 were considered simultaneously, the minimum residence time would be 277 h, and the concentration of CHCl_3 would be $59.8 \mu\text{g/L}$, which was lower than the maximum allowable concentration. Therefore, the generation and degradation of CHCl_3 would be the determining factor when determining minimum residence time.

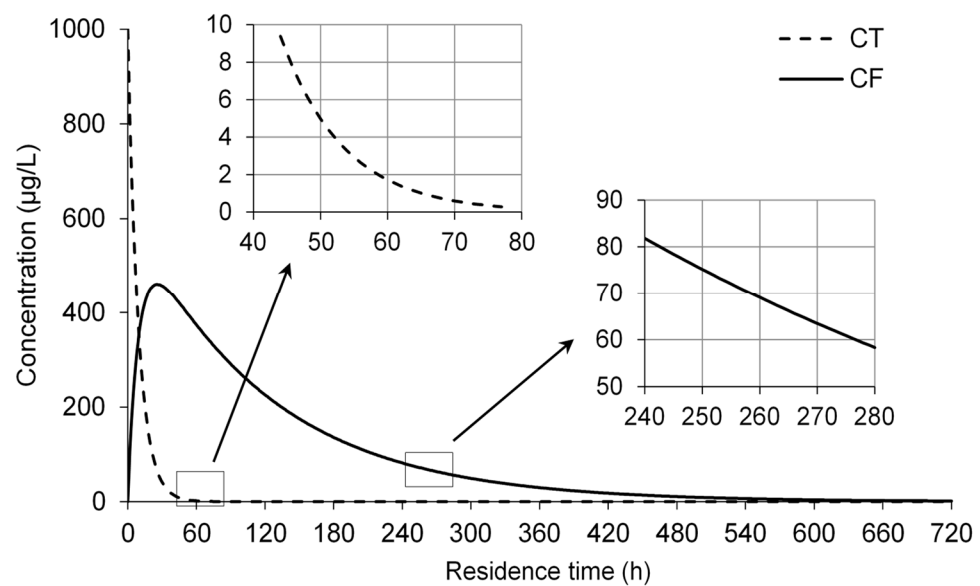


Figure 9. Changes in CCl₄ concentration and its degradation products in the ZVI-water system. Assuming that initial CCl₄ and CHCl₃ concentrations were 1000 µg/L and 0.0 µg/L and $k_{obs,CT}$ and $k_{obs,CF}$ were 0.1139 h⁻¹ and 0.0109 h⁻¹, respectively.

4. Conclusions

Sponge ZVI particles can effectively degrade CCl₄ in groundwater, which followed pseudo first-order reaction kinetics. The pseudo first-order reaction rate constant (k_{obs}) of CCl₄ was 0.1139 h⁻¹ at a ZVI dosage of 20 g/L and an initial CCl₄ concentration of 20 mg/L. During the degradation process, approximately 75% of CCl₄ was transformed to CHCl₃ by hydrogenolysis. The transformation of CHCl₃ in the ZVI-H₂O system was relatively slow, with the k_{obs} of CHCl₃ being 0.0109 h⁻¹. Therefore, the minimum residence time was controlled by the production and subsequent transformation of CHCl₃ for the ZVI-based PRB.

The main factors affecting CCl₄ degradation by ZVI were the dosage of ZVI and the solution pH. CCl₄ degradation was promoted when the ZVI dosage was increased and the k_{obs} of CCl₄ increased linearly with ZVI dosages from 0 to 40 g/L. The calculated surface-area-normalized reaction rate constants for the various dosages indicated the optimum ZVI dosage as 20 g/L. The weakly acidic conditions facilitated the degradation of CCl₄, and the k_{obs} of CCl₄ decreased linearly for pH range of 5–8. Surface acidic washing had no significant effect on CCl₄ removal by ZVI.

Author Contributions: Conceptualization, X.Z. and Q.F.; methodology, L.Z.; validation, X.Z. and B.H.; formal analysis, X.Z.; investigation, X.Z.; data curation, X.Z.; writing—original draft preparation, X.Z. and Q.F.; writing—review and editing, Y.L.; supervision, B.H.; funding acquisition, X.Z. All authors have read and agreed to the published version of the manuscript.

Funding: This work was financially supported by the National Key Research and Development Project of China (Grant No. 2020YFC1806502).

Institutional Review Board Statement: Not applicable.

Informed Consent Statement: Not applicable.

Data Availability Statement: The data presented in this study are available on request from the corresponding author.

Conflicts of Interest: The authors declare that they have no known competing financial interests or personal relationships that could have appeared to influence the work reported in this paper.

References

1. Tang, P.; Jiang, W.; Lyu, S.; Brusseau, M.L.; Xue, Y.; Qiu, Z.; Sui, Q. Mechanism of carbon tetrachloride reduction in ferrous iron activated calcium peroxide system in the presence of methanol. *Chem. Eng. J.* **2019**, *362*, 243–250. [[CrossRef](#)]
2. Alvarado, J.S.; Rose, C.; LaFreniere, L. Degradation of carbon tetrachloride in the presence of zero-valent iron. *J. Environ. Monitor.* **2010**, *8*, 1524–1530. [[CrossRef](#)] [[PubMed](#)]
3. Penny, C.; Gruffaz, C.; Nadalig, T.; Cauchie, H.M.; Vuilleumier, S.; Bringel, F. Tetrachloromethane-degrading bacterial enrichment cultures and isolates from a contaminated aquifer. *Microorganisms* **2015**, *3*, 327–343. [[CrossRef](#)] [[PubMed](#)]
4. Davis, G.G.; Peck, F.C. Degradation of carbon tetrachloride in a reducing groundwater environment: Implications for natural attenuation. *Appl. Geochem.* **2003**, *18*, 503–525. [[CrossRef](#)]
5. U.S. Environmental Protection Agency. *IRIS Toxicological Review of Carbon Tetrachloride (Final Report)*; U.S. Environmental Protection Agency: Washington, DC, USA, 2010.
6. Gee, G.W.; Oostrom, M.; Freshley, M.D.; Rockhold, M.L.; Zachara, J.M. Hanford site vadose zone studies: An overview. *Vadose Zone J.* **2007**, *4*, 899–905. [[CrossRef](#)]
7. Huang, B.; Lei, C.; Wei, C.; Zeng, G. Chlorinated volatile organic compounds (Cl-VOCs) in environment—sources, potential human health impacts, and current remediation technologies. *Environ. Int.* **2014**, *71*, 118–138. [[CrossRef](#)]
8. Dominguez, C.M.; Rodriguez, V.; Montero, E. Methanol-enhanced degradation of carbon tetrachloride by alkaline activation of persulfate: Kinetic model. *Sci. Total Environ.* **2019**, *666*, 631–640. [[CrossRef](#)]
9. O'Carroll, D.; Sleep, B.; Krol, M.; Boparai, H.; Kocur, C. Nanoscale zero valent iron and bimetallic particles for contaminated site remediation. *Adv. Water Resour.* **2013**, *51*, 104–122. [[CrossRef](#)]
10. Lefevre, E.; Bossa, N.; Wiesner, M.R.; Gunsch, C.K. A review of the environmental implications of in situ remediation by nanoscale zero valent iron (nZVI): Behavior, transport and impacts on microbial communities. *Sci. Total Environ.* **2016**, *565*, 889–901. [[CrossRef](#)]
11. He, F.; Gong, L.; Fan, D.; Tratnyek, P.G.; Lowry, G.V. Quantifying the efficiency and selectivity of organohalide dechlorination by zerovalent iron. *Environ. Sci.-Proc. Imp.* **2020**, *3*, 528–542. [[CrossRef](#)]
12. Velimirovic, M.; Larsson, P.-O.; Simons, Q.; Bastiaens, L. Reactivity screening of microscale zerovalent irons and iron sulfides towards different CAHs under standardized experimental conditions. *J. Hazard. Mater.* **2013**, *252–253*, 204–212. [[CrossRef](#)] [[PubMed](#)]
13. Comba, S.; Di Molfetta, A.; Sethi, R. A comparison between field applications of nano-, micro-, and millimetric zero-valent iron for the remediation of contaminated aquifers. *Water Air Soil Pollut.* **2011**, *1–4*, 595–607. [[CrossRef](#)]
14. Velimirovic, M.; Larsson, P.-O.; Simons, Q.; Bastiaens, L. Effect of boron on reactivity and apparent corrosion rate of microscale zerovalent irons. *J. Environ. Chem. Eng.* **2017**, *2*, 1892–1898. [[CrossRef](#)]
15. Velimirovic, M.; Auffan, M.; Carniato, L.; Batka, V.M.; Schmid, D.; Wagner, S.; Borschneck, D.; Proux, O.; Kammer, F.; Hofmann, T. Effect of field site hydrogeochemical conditions on the corrosion of milled zerovalent iron particles and their dechlorination efficiency. *Sci. Total Environ.* **2018**, *618*, 1619–1627. [[CrossRef](#)]
16. Zhu, X.; Han, B.; Feng, Q. Common Anions Affected Removal of Carbon Tetrachloride in Groundwater Using Granular Sponge Zerovalent Iron. *Water Air Soil Pollut.* **2020**, *4*, 1–13. [[CrossRef](#)]
17. Bae, S.; Lee, W. Influence of riboflavin on nanoscale zero-valent iron reactivity during the degradation of carbon tetrachloride. *Environ. Sci. Technol.* **2014**, *4*, 2368–2376. [[CrossRef](#)]
18. Orth, W.S.; Gillham, R.W. Dechlorination of trichloroethene in aqueous solution using Fe⁰. *Environ. Sci. Technol.* **1995**, *1*, 66–71. [[CrossRef](#)]
19. Johnson, T.L.; Scherer, M.M.; Tratnyek, P.G. Kinetics of halogenated organic compound degradation by iron metal. *Environ. Sci. Technol.* **1996**, *8*, 2634–2640. [[CrossRef](#)]
20. Alowitz, M.J.; Scherer, M.M. Kinetics of nitrate, nitrite, and Cr (VI) reduction by iron metal. *Environ. Sci. Technol.* **2002**, *3*, 299–306. [[CrossRef](#)]
21. Lai, K.C.K.; Lo, I.M.C. Removal of chromium (VI) by acid-washed zero-valent iron under various groundwater geochemistry conditions. *Environ. Sci. Technol.* **2008**, *4*, 1238–1244. [[CrossRef](#)]
22. Phenrat, T.; Lowry, G.V.; Babakhani, P. *Nanoscale Zerovalent Iron (NZVI) for Environmental Restoration: From Fundamental Science to Field Scale Engineering Applications*; Springer International Publishing: Cham, Switzerland, 2019.
23. Xin, J.; Zheng, X.; Han, J.; Shao, H.; Kolditz, O. Remediation of trichloroethylene by xanthan gum-coated microscale zero valent iron (XG-mZVI) in groundwater: Effects of geochemical constituents. *Chem. Eng. J.* **2015**, *271*, 164–172. [[CrossRef](#)]
24. Helland, B.R.; Alvarez, P.J.J.; Schnoor, J.L. Reductive dechlorination of carbon tetrachloride with elemental iron. *J. Hazard. Mater.* **1995**, *2*, 205–216. [[CrossRef](#)]
25. Lin, Y.T.; Liang, C. Carbon Tetrachloride Degradation by Alkaline Ascorbic Acid Solution. *Environ. Sci. Technol.* **2013**, *7*, 3299–3307. [[CrossRef](#)] [[PubMed](#)]
26. Dolfing, J.; Mueller, J. Thermodynamics of low Eh reactions. In Proceedings of the Bettelle's Fifth International Conference on Remediation of Chlorinated and Recalcitrant Compounds, Monterey, CA, USA, 22–26 May 2006.
27. Cwiertny, D.M.; Scherer, M.M. Abiotic Processes affecting the remediation of chlorinated solvents. In *In Situ Remediation of Chlorinated Solvent Plumes*; Stroo, H.F., Ward, C.H., Eds.; Springer: New York, NY, USA, 2010; pp. 69–108.

28. Puls, R.W.; Blowes, D.W.; Gillham, R.W. Long-term performance monitoring for a permeable reactive barrier at the U.S. Coast Guard Support Center, Elizabeth City, North Carolina. *J. Hazard. Mater.* **1999**, *1–2*, 109–120. [[CrossRef](#)]
29. Jin, X.; Chen, H.; Yang, Q.; Hu, Y.; Yang, Z. Dechlorination of Carbon Tetrachloride by Sulfide-Modified Nanoscale Zerovalent Iron. *Environ. Eng. Sci.* **2018**, *6*, 560–567. [[CrossRef](#)]
30. Jiao, Y.; Qiu, C.; Huang, L.; Wu, K.; Ma, H.; Chen, S.; Ma, L.; Wu, D. Reductive dechlorination of carbon tetrachloride by zero-valent iron and related iron corrosion. *Appl. Catal. B-Environ.* **2009**, *1–2*, 434–440.
31. Shih, Y.H.; Hsu, C.Y.; Su, Y.F. Reduction of hexachlorobenzene by nanoscale zero-valent iron: Kinetics, pH effect, and degradation mechanism. *Separ. Purif. Technol.* **2011**, *3*, 268–274. [[CrossRef](#)]
32. Bae, S.; Hanna, K. Reactivity of nanoscale zero-valent iron in unbuffered systems: Effect of pH and Fe(II) dissolution. *Environ. Sci. Technol.* **2015**, *17*, 10536–10543. [[CrossRef](#)]
33. Tang, F.; Xin, J.; Zheng, X.; Zheng, T.; Yuan, X.; Kolditz, O. Effect of solution pH on aging dynamics and surface structural evolution of mZVI particles: H₂ production and spectroscopic/microscopic evidence. *Environ. Sci. Pollut. R.* **2017**, *30*, 23538–23548. [[CrossRef](#)]
34. Liu, W.J.; Qian, T.T.; Jiang, H. Bimetallic Fe nanoparticles: Recent advances in synthesis and application in catalytic elimination of environmental pollutants. *Chem. Eng. J.* **2014**, *236*, 448–463. [[CrossRef](#)]
35. Huang, Q.; Liu, W.; Peng, P.; Huang, W. Reductive dechlorination of tetrachlorobisphenol A by Pd/Fe bimetallic catalysts. *J. Hazard. Mater.* **2013**, *262*, 634–641. [[CrossRef](#)] [[PubMed](#)]
36. Dong, J.; Zhao, Y.; Zhao, R.; Zhou, R. Effects of pH and particle size on kinetics of nitrobenzene reduction by zero-valent iron. *J. Environ. Sci.* **2010**, *11*, 1741–1747. [[CrossRef](#)]
37. Williams, A.G.B.; Scherer, M.M. Spectroscopic evidence for Fe (II)-Fe (III) electron transfer at the iron oxide-water interface. *Environ. Sci. Technol.* **2004**, *18*, 4782–4790. [[CrossRef](#)] [[PubMed](#)]
38. Obiri-Nyarko, F.; Grajales-Mesa, S.J.; Malina, G. An overview of permeable reactive barriers for in situ sustainable groundwater remediation. *Chemosphere* **2014**, *111*, 243–259. [[CrossRef](#)] [[PubMed](#)]